GPO PRICE $ _____

CFSTI PRICE(S) $ _____

Hard copy (HC) 3.00

Microfiche (MF) .65

ff 653 July 65

N68-27456 (ACCESSION NUMBER) (THRU)
39 (PAGES) 1 (CODE)
TMX-63242 (NASA CR OR TMX OR AD NUMBER) 14 (CATEGORY)
FACILITY FORM 602

X-611-68-221
PREPRINT

NASA TM X-63242

EFFECTS OF DAMAGE BY 0.8 MeV-5.0 MeV PROTONS IN SILICON SURFACE — BARRIER DETECTORS

J. A. COLEMAN
D. P. LOVE
J. H. TRAINOR
D. J. WILLIAMS

JUL 1968
RECEIVED
NASA STI FACILITY
INPUT BRANCH

JUNE 1968

GSFC

GODDARD SPACE FLIGHT CENTER
GREENBELT, MARYLAND

611-68-221
Preprint

EFFECTS OF DAMAGE BY 0.8 MeV - 5.0 MeV PROTONS IN SILICON SURFACE - BARRIER DETECTORS

J. A. Coleman
National Bureau of Standards, Washington, D. C.

D. P. Love
Vitro Services, Goddard Space Flight Center

J. H. Trainor and D. J. Williams
NASA/Goddard Space Flight Center
Greenbelt, Md.

June 1968

EFFECTS OF DAMAGE BY 0.8 MeV - 5.0 MeV PROTONS IN SILICON SURFACE - BARRIER DETECTORS

SUMMARY

Changes in the performance of silicon surface - barrier detectors after irradiation with protons at energies between 0.80 MeV and 5.00 MeV have been investigated for fluences up to 10^{17} protons cm^2. Irradiations of the front, surface - barrier contacts and the rear, ohmic contacts of these transmission detectors were performed. In general, the detector current and noise increased with fluence. When the rear, ohmic contact was irradiated with protons which stopped within the detector, the changes in the current and noise after irradiation were several orders of magnitude smaller than after a similar irradiation of the front contact. For protons with energies greater than about 1 MeV, the detector capacitance decreased at low reverse biases and increased at high biases with increasing fluence. The results indicate that a significant reduction in the increase of detector current and noise can be obtained if the density of radiation - produced defects in the region of the junction is minimized.

INTRODUCTION

Silicon nuclear radiation detectors operating on Earth-orbiting satellites and deep space probes can be destroyed by high fluxes of low - energy protons which exist in the trapped - radiation belts or which arise from transient solar events. The useful lifetime of detectors which must operate in such environments depends on the flux and energy of protons which cause the radiation damage. In addition to detector lifetime predictions, a study of radiation damage effects in detector structure can be useful for the intelligent interpretation of data from detectors subjected to intense particle fluxes.

The effects of damage in totally-depleted, silicon, surface - barrier detectors by protons with energies between 50 keV and 1.00 MeV for fluences up to 10^{14} cm^{-2} have been reported recently.[1] This study showed that irradiation of the front, surface - barrier contact with low - energy protons produced an increase in the detector reverse - biased current, noise, and capacitance with fluence. Significant increases in current and noise occurred at fluences greater than about 10^{13} protons cm^{-2}. Damage effects were reduced by several orders of magnitude if the rear, ohmic contact, rather than the front, surface barrier contact, of the totally - depleted detectors was irradiated with short - range protons. Also evident in these earlier results was the high concentration of defects created at the end of the proton range. This arises from the fact that the silicon atom displacement

cross-section is inversely proportional to the proton energy. It was observed that the intense proton end - of - range damage produced an increase in the net space - charge density in the high resistivity n-type silicon from which the detectors were made, indicating that the damage sites were acting as donor - type inpurity centers.

The results reported here confirm the earlier study and extend the available data on proton damage effects in surface - barrier silicon detectors to proton energies of 5 MeV. New and confirmatory data is also presented on the significant reduction of proton damage effects which can be obtained by irradiation of the rear, ohmic contact rather than the front, surface - barrier contact of these detectors. The results of this study are presented so that an experimenter might easily use the data to predict changes in the performance of detectors operating in similar radiation environments.

EQUIPMENT AND PROCEDURES

The detectors, irradiation procedures and measurements employed for this study are similar to those which were described in detail in the previous work.[1] The silicon, surface - barrier, transmission detectors had nominal thicknesses and areas of 100 m and 50 mm^2, respectively. The wafers used in the detectors were cut from an ingot 1700 - 2200 ohm - cm, n-type (phosphorus-doped) silicon which had a photoconductive decay lifetime of 2500 sec. Total depletion

of the detectors was achieved at reverse biases of 25 - 30V, and the maximum operating biases were 45 - 60V.

The irradiation of two detectors at each proton energy in the previous study had demonstrated that reproducible results could be obtained with the experimental procedures which were used. In the study reported here only one detector was irradiated at each energy. Details of the irradiations including the proton energies, the proton ranges in silicon,[2] the detector thicknesses,[7] and the contact which was irradiated are tabulated in Table 1 and illustrated in Fig. 1.

The proton beam was collimated so that a 5mm diameter area at the center of the detector's sensitive area was irradiated. The beam intensity on the detector was measured by inserting a small Faraday cup between the beam collimator and the detector. After the beam was stabilized, the currents in the Faraday cup and on the collimators were measured. The Faraday cup was removed during the irradiations and the beam stability was monitored by noting the constancy of collimator current. The arrangement of the detectors, Faraday cup and alpha particle sources in the vacuum chamber is shown in Fig. 2. The proton fluxes used ranged from 1×10^{10} to 3×10^{12} protons cm^{-2} sec^{-1} except for the 0.8 MeV rear contact irradiation which was at a flux of 3.5×10^{13} protons cm^{-2} sec^{-1}. The flux was kept constant to $\pm$ 5% for each irradiation. The detectors were mounted in the irradiation chamber, which was at

the ambient temperature of approximately 25°C. A vacuum of approximately 10^{-5} torr was maintained within the chamber throughout all the irradiations and testing at a given proton energy. Each detector was biased at its maximum operating voltage at the start of each irradiation and the detector current was monitored during the irradiation. Heating of the detectors by the beam was not considered to be significant (< 2°C) for any irradiation except for the final two irradiations at 5 MeV.

After each irradiation, the detector current, noise, capacitance and counting response to Am-241 alpha particles incident on both contacts were measured as a function of reverse bias. The noise and counting measurements were made using an amplifier system with 0.8 sec double integration and double differentiation time constants. Since the alpha particle source was placed directly in front of the beam collimator during the counting measurements, an area slightly larger than the radiation-damaged area was exposed to alpha particles.

At proton fluences greater than about 10^{14} cm^{-2}, detector characteristics were not measured until the current and noise had stabilized; usually this occurred within a few hours for the irradiations reported here. Since heating effects by the proton beams was considered to be negligible except for the 5 MeV irradiation, it was felt that the rapid reduction of current and noise after large proton fluences was due to the rapid annealing of defects.

RESULTS

The results of the post-irradiation detector measurements are presented in a manner to emphasize the changes of detector performance with fluence and proton energy, and to contrast the difference between damage effects by protons incident on the front, surface - barrier contact and on the rear, ohmic contact. Although measurements were taken for proton irradiations at about 2 MeV, the detailed results are not presented since they can be estimated by interpolating between the 0.8 MeV and 3 MeV results. In all the irradiations except at 4.5 MeV and 5.0 MeV, the protons stopped in the detector. The position of the intensive end-of-range damage with respect to the high-field, junction region of the detectors should be considered when reviewing the results presented below.

Detector current-voltage characteristics measured after various proton fluences are shown in Figs. 3 and 4 for the irradiation of the front and rear contacts with 0.8 MeV and 3 MeV protons. It is evident that irradiation of the rear, ohmic contact provided relatively low-current operation and, as will be shown later, low-noise operation of these detectors for several orders of magnitude more in fluence than corresponding irradiations of the front, junction contact. Note also that the 0.8 MeV protons produced much smaller damage effects than the 3.0 MeV protons. When higher energy protons passed through the detectors without stopping, the current-voltage characteristics at a given fluence were similar for both the front and the rear irradiations,

as shown in Fig. 5. In these irradiations at 4.5 MeV and 5.0 MeV the energies of the protons near the surface-barrier were similar and, thus, the density and type of defects formed near the junction are expected to be similar. After 5×10^{13} protons cm^{-2} the current-voltage characteristic for the 5 MeV rear-contact irradiation was slightly higher than for the 4.5 MeV front contact bombardment. Perhaps this reflects the fact that in the 5 MeV irradiation the proton energies at the junction were slightly smaller than in the 4.5 MeV irradiation (see Fig. 1). The silicon atom displacement corss-section varies inversely with the proton energy. Except for the 0.8 MeV irradiations, the currents at the lowest bias voltages increased sharply with increasing fluence. This effect may relate to the difference in the type ofdefects which are formed at proton energies below and above about 1 MeV.

The detector current increase at maximum detector bias as a function of fluence is shown in Fig. 6 for different proton energies. Except for the highest energy irradiations, the current increase is larger for the higher proton energies, regarless of which contact was irradiated. However, the advantage of irradiating the rear, ohmic contact in the case of short-range protons is obvious. For the front-contact irradiations, the current increases are nearly proportional to the fluence.

The detector noise as a function of applied reverse bias for various fluences is given in Figs. 7, 8 and 9 for the three proton energies mentioned above. The general trends are similar to those

in the current measurements.

The effect of decreasing detector capacitance and a subsequent lowering of the noise with bias is evident in most of the figures for biases up to about 15V. At high fluences and high biases microplasma-type (mp) noise was observed in some detectors. A summary of the increase of noise with fluence for various proton energies is shown in Fig. 10. When the front contact was irradiated, the noise increased approximately as the square root of the fluence. A comparison of the current increase and the noise increase with fluence shows that, for the front-contact irradiations, the detectors with the higher currents tended to have the lower noise values. For the irradiations at proton energies below 1 MeV the opposite effect had been observed, lower noise for lower currents.[1] Perhaps at the higher proton energies the noise spectrum changes as different types and densities of defects are produced. Unlike the irradiations at proton energies below 1 MeV, the detector noise for these higher energy irradiations does not increase sharply at fluences above 10^{14} protons cm^{-2}. This may reflect the fact that smaller defect densities are produced in the high field region near the junction for proton energies greater than about 1 MeV.

The earlier study showed that the detector capacitance increased with fluence after irradiation of the front contacts with protons of energies less than 1 MeV. However, the increase of the capacitance was larger for the lower energy bombardments. The capacitance-voltage

characteristics for various fluence values after irradiation with 0.8 MeV protons are shown in Fig. 11. Short-range protons (See Fig. 1) produced large changes in the capacitance when the junction contact was irradiated and negligible capacitance changes when the rear, ohmic contact was irradiated. In general, the capacitance values after irradiation of the front contact were dependent on the fluence and the position of the end-of-range damage with respoect to the surface- barrier junction.

With 3 MeV protons (Fig. 12) and 5 MeV protons (Fig. 13), the capacitance decreased with fluence at biases below about 10V and increased at higher biases when the front contact was irradiated. Irradiation of the rear contact produced capacitance changes which appeared to depend on the location of the end-of-range damage with respect to the junction. A summary of the capacitance-voltage characteristics for similar fluences with different proton energies incident on the front and rear contacts is shown in Fig. 14. The position of the end-of-range damage with respect to the junction appears to determine the magnitude of the capacitance values. In the front-contact irradiations, the change in the detector capacitance was larger for the shorter range protons, whereas in the rear-contact irradiations the opposite order was observed.

The analysis of spectra from counting Am-241 alpha particles after proton damage indicated the following: presence of depletion depths which were smaller than the range of the alpha particles,

damaged regions with poor collection efficiency, and undepleted layers near the rear contact even at 50 percent over-bias. The effects on the counting response of detectors after irradiation by 0.8 MeV protons on the front and on the rear contacts are shown in Figs. 15 and 16, respectively. The full-energy peak at about 5.5 MeV usually is the result of alpha particles entering the undamaged peripheral region around the central damaged spot. A thin deplection region with a low lifetime causes the lower energy peaks in Fig. 15. The source of the lower energy peaks at 12V and 25V in Fig. 16 is not understood. Capacitance measurements (see Fig. 11) indicate that at these bias voltages, the detector is less than 50 percent depleted in the damaged area. The high lifetime of the undepleted region near the back contact may allow the diffusion of some carriers to the high field region, thus producing smeared, low-energy peaks.

The low-energy peaks after rear-contact damage as shown in Fig. 17 appear to be caused by the fact that the thin, damaged layer at the back contact was undepleted even at the highest bias. Charge collection problems for alpha particles incident on the front contact after proton damage to the rear contact are minimal at this fluence of 5.1×10^{13} cm^{-2}. However, at a fluence of 1.6×10^{14} 0.8 MeV protons cm^{-2} incident on the rear contact, distinctly separate peaks were observed for alpha particles incident on the front contact. This effect may be caused by the high resistance of the ohmic rear contact after extensive proton damage. Signals from carriers traversing the detector to the damaged region at the back may be slower due to the

large contact resistance. This large resistance at the rear contact after damage may also be manifested in Figs. 3 and 4 where current values, in some cases, were smaller for larger fluences. In these cases the voltage applied across the junction may have been significantly reduced by the voltage drop across the damaged rear contact.

Alpha particle spectra after the irradiation of the front and rear contacts at similar fluences of 2.78 MeV and 3.00 MeV protons are shown in Figs. 18 and 19 respectively. The lower energy peaks for alpha particles incident on the front contacts appear to be caused mainly by trapping effects. For alpha particles incident on the rear contact, dead-layers resulting from undepleted regions at the rear contact appear to cause the lower energy peaks (see Fig. 12).

Strikingly different alpha particle spectra were observed after 2.5×10^{14} 4.5 MeV protons cm^{-2} as shown in Fig. 20. Severe trapping effects causing poor charge collection were observed for alpha particles incident on the front contact. However, only a dead-layer effect was observed for alpha particles incident on the rear contact. This was expected since the detector was not fully depleted (see Fig. 13). When alpha particles entered the front contact, electrons had to make the major traversal of the depletion region. Perhaps these observations indicate that defects produced by these higher energy protons cause the selective trapping of electrons rather than holes.

DISCUSSION

The interaction between protons and silicon nuclei in a detector occurs predominately by the Rutherford scattering process. In this

process the cross-section for the displacement of a silicon atom is inversely proportional to the proton energy. Therefore the density of defects produced near the end of the proton track rises very sharply. Dearnaley has calculated the total number of defects produced in each unit interval of the proton track.[3] His results show that the linear density of defects produced by protons in silicon rises sharply at energies below about 2 MeV. In addition, Dearnaley has estimated that the total number of Frenkel defects (vacancy and nearby interstitial) produced by a proton in silicon si given by

$$N_F = 130 + 6\ E_P,$$

where E_P is the proton energy in MeV. This illustrates the relative importance of the end-of-track damage in terms of defect production for protons with energies of several MeV.

In general, this study and the previous one have shown that the effects of damage by protons which stop in silicon detectors are dominated by the intense end-of-range production of defects. The position of the end-of-range damage with respect to the high field region at the surface-barrier junction and the type of defect sites formed along the track are most important in determining the response of silicon surface-barrier detectors after damage by low-energy protons. When the protons do not stop in the detector depletion regions, the energy dependence of the damage is minimized.

The results of these studies of low-energy proton damage in silicon detectors indicate that the end-of-range damage sites act as

donor-type defects. However, the defects produced protons with energies above about 1 MeV tended to decrease the net space-charge density in the n-type silicon from which the detectors were made. This can be readily seen in the changes of the detector capacitances as the proton energy was increased. When the surface-barrier contact was irradiated with very low-energy protons the capacitance was very large at all bias voltages. As the proton energy was raised above 1 MeV, the capacitance decreased with fluence at low biases, indicating that the effective resistivity of the silicon near the junction has increased. At higher biases the capacitance increased with fluence, indicating that a layer of donor-type defects was encountered deeper in the detector.

The mechanism for the creation of acceptor-type defects at the beginning, and donor-type defects at the end of the track of a proton with an energy greater than about 1 MeV is not understood at the present time. The type of defect which is formed may depend on the mean energy of the recoiling silicon atoms and/or the distribution of the defects. The mean energy of the recoils is proportional to the logarithm of the energy of the proton, thus decreasing as the proton is slowed in the silicon. The density of defects becomes very large at the end of the proton track, thus enhancing the probability of defect-defect interactions. A study of these possible mechanisms is anticipated.

For low-noise operation of surface-barrier transmission detectors which are exposed to short-range protons, the advantages of irradiating the rear, ohmic contact have been clearly demonstrated by these studies. In addition, it is important to keep the density of defects as small as possible in the junction or high field region of the detectors. If collection of charge is important, high field operation of the detectors is a necessity to insure full depletion-depths and to minimize the loss of charge due to trapping on damage sites. However, operating a detector with a high electric field in order to reduce the effects of radiation damage can be detrimental. For example, leakage currents and noise increase sharply with fluence at high detector biases. In addition, the depletion depth of the detector may be reduced as more voltage is dropped across the bias load resistor.

Experimenters must choose carefully the type of detector and the operating conditions when using semiconductor detectors in high-flux radiation environments.

Acknowledgements

The assistance during the irradiations of S. Brown, GSFC, and P.R. Malmberg and the crew of the Naval Research Laboratory Van de Graff accelerator is gratefully acknowledged.

REFERENCES

1. J. A. Coleman, D. P. Love, J. H. Trainor and D. J. Williams, "Low-Energy Proton Damage Effects in Silicon Surface-Barrier Detectors", Proceedings of the 14th Nuclear Science Symposium, October 31-November 2, 1967 (to be published).

2. J. F. Janni, "Calculations of Energy Loss, Range, Pathlength, Straggling, Multiple-Scattering and the Probability of Inelastic Nuclear Collisions for 0.1-1000 MeV Protons", Technical Report No. AFWL-TR-65-150, Kirtland Air Force Base, New Mexico, 1966.

3. G. Dearnaley, "Radiation Damage by Charged Particles in Silicon Junction Detectors", IEEE Trans. Nucl. Sci., NS-10, 106 (1963).

TABLE 1. Proton ranges in silicon and detector thicknesses

PROTON ENERGY (MeV)	RANGE IN SILICON (μm)	DETECTOR	DETECTOR THICKNESS (μm)	CONTACT
0.80	12.7	6-168C	81	Front (Au)
0.80	12.7	6-777B	129	Rear (Al)
1.85	43.1	6-781B	133	Front
2.00	48.5	6-170C	93	Rear
2.78	81.9	7- 59B	102	Front
3.00	92.7	6-780B	117	Rear
4.50	181.2	6-784B	119	Front
5.00	216.2	6-165C	81	Rear

5.48 MeV alpha particle (Am-241) range in Si is $\sim$ 28 m

FIGURE CAPTIONS

1. Schematic illustration of the proton ranges in the silicon detectors used in the irradiations.

2. Top view of the irradiation chamber showing the detector mount, collimators and alpha particle sources.

3. Current-voltage characteristics after various fluences of 0.80 MeV protons incident on the front surface-barrier contact of detector 6-168C and on the rear, ohmic contact of detector 6-777B.

4. Detector current-voltage characteristics after various fluences of 2.78 MeV protons (front entry) and 8.00 MeV protons (rear entry).

5. Detector current-voltage characteristics after various fluences of 4.50 MeV protons (front entry) and 5.00 MeV protons (rear entry).

6. The increase of detector current at the maximum reverse bias as a function of proton fluence for front and rear contact irradiations at several energies between 0.80 MeV and 5.00 MeV. The values represented by points marked A were measured 12 hours after the irradiations.

7. Noise-voltage characteristics after various fluences of 0.80 MeV protons incident on the front contact and rear contact of different detectors. The noise is expressed in keV full-width-half-maximum (FWHM) of a Gaussian distribution. Microplasma observations are indicated by mp.

8. Detector noise-voltage characteristics after various fluences of 2.78 MeV protons (front entry) and 3.00 MeV (rear entry).

9. Detector noise-voltage characteristics after various fluences of 4.50 MeV protons (front entry) and 5.00 MeV protons (rear entry).

10. Total system noise at the maximum detector reverse bias as a function of proton fluence for front and rear contact irradiations at several energies between 1.85 MeV and 5.00 MeV.

11. Detector capacitance-voltage characteristics after various fluences of 0.80 MeV protons incident on the front contact and rear contact of different detectors.

12. Detector capacitance-voltage characteristics after various fluences of 2.78 MeV protons (front entry) and 3.00 MeV protons (rear entry).

13. Detector capacitance-voltage characteristics after various fluences of 4.50 MeV protons (front entry) and 5.00 MeV protons (rear entry).

14. A comparison of detector capacitance-voltage characteristics for front and rear entry irradiations at similar proton fluences for several energies between 0.80 MeV and 5.00 MeV.

15. Spectra resulting from alpha particles entering the front contact at three detector reverse biases after irradiation of the front contact by 5.1×10^{13} 0.80 MeV protons cm^{-2}.

16. Spectra resulting from alpha particles entering the rear contact at three detector reverse biases after irradiation of the front contact by 5.1×10^{13} 0.80 MeV protons cm^{-2}.

17. Spectra resulting from alpha particles entering the front and rear contacts at two detector reverse biases after irradiation of the rear contact by 5.1×10^{13} 0.80 MeV protons cm^{-2}.

18. Spectra resulting from alpha particles entering the front and rear contacts at two detector reverse biases after irradiation of the front contact by 4.6×10^{13} 2.78 MeV protons cm^{-2}.

19. Spectra resulting from alpha particles entering the front and rear contacts at two detector reverse biases after irradiation of the rear contact by 2.4×10^{13} 3.00 MeV protons cm^{-2}.

20. Spectra resulting from alpha particles entering the front and rear contacts at two detector reverse biases after irradiation of the front contact with 2.5×10^{14} 4.50 MeV protons cm^{-2}.

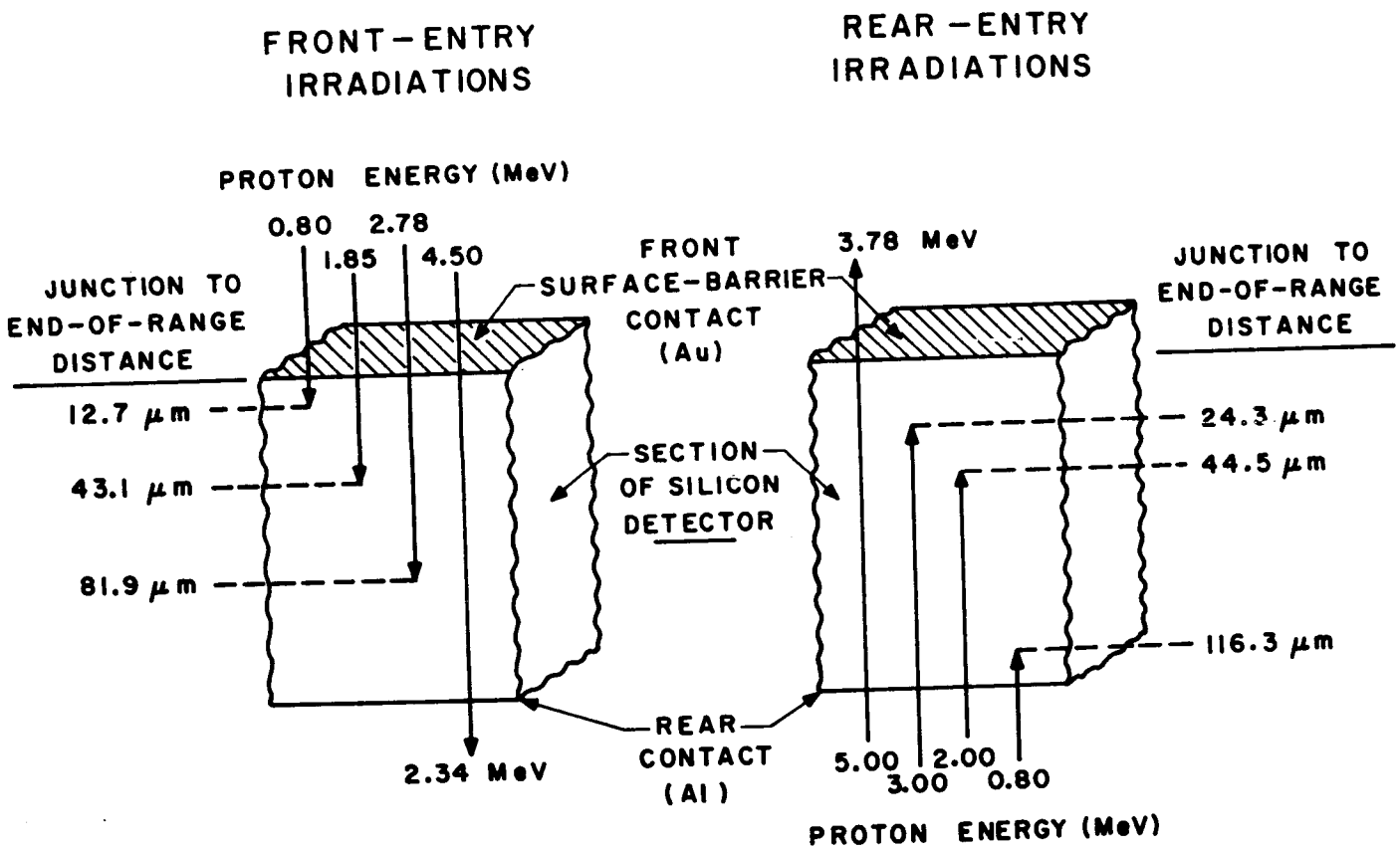
FRONT-ENTRY IRRADIATIONS
REAR-ENTRY IRRADIATIONS
PROTON ENERGY (MeV)
0.80
2.78
1.85
4.50
JUNCTION TO END-OF-RANGE DISTANCE
12.7 μm
43.1 μm
81.9 μm
FRONT SURFACE-BARRIER CONTACT (Au)
SECTION OF SILICON DETECTOR
REAR CONTACT (Al)
2.34 MeV
3.78 MeV
JUNCTION TO END-OF-RANGE DISTANCE
24.3 μm
44.5 μm
116.3 μm
5.00
3.00
2.00
0.80
PROTON ENERGY (MeV)

FIG. 1

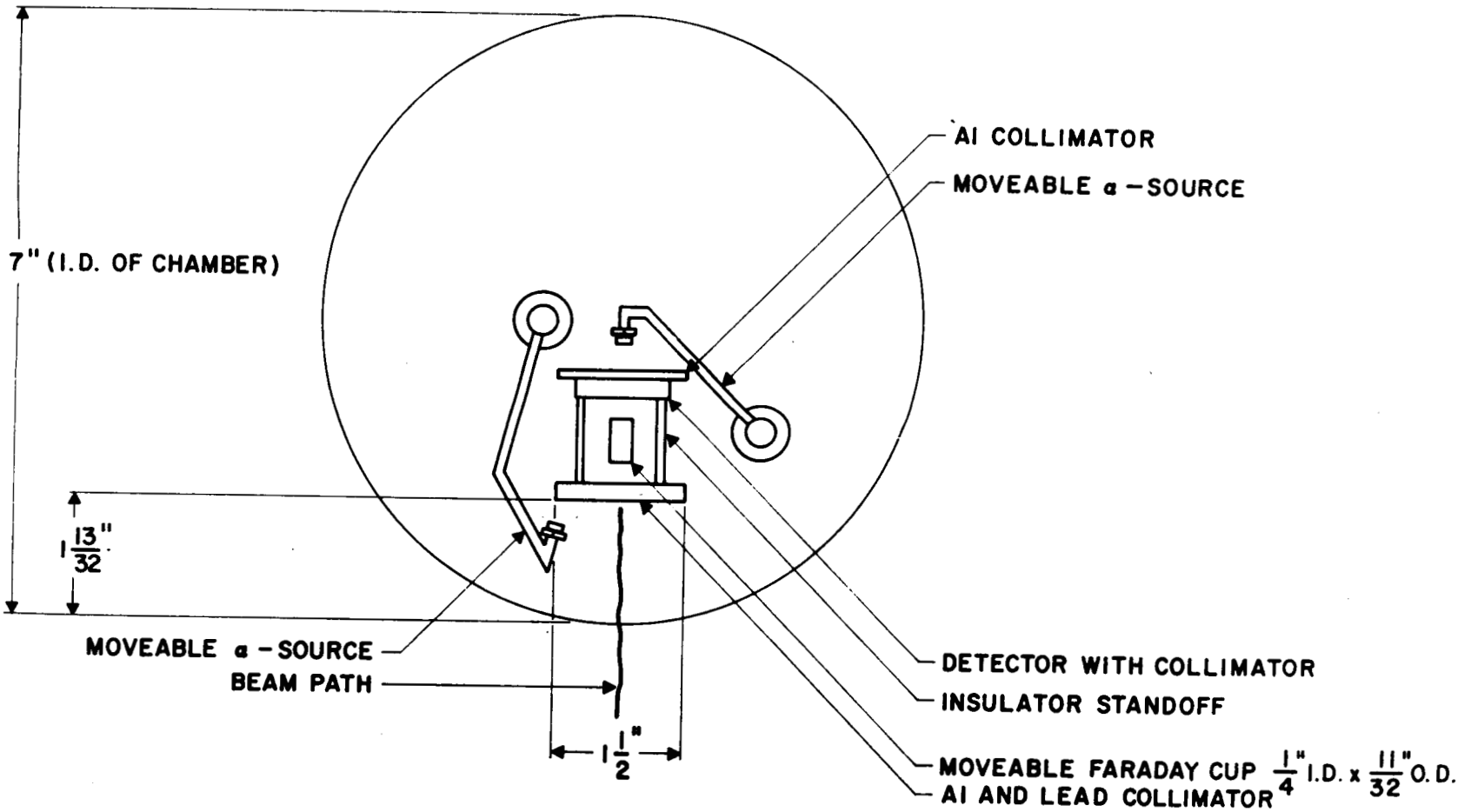
7" (I.D. OF CHAMBER)
1 13/32"
Al COLLIMATOR
MOVEABLE α -SOURCE
MOVEABLE α -SOURCE
BEAM PATH
1 1/2"
DETECTOR WITH COLLIMATOR
INSULATOR STANDOFF
MOVEABLE FARADAY CUP 1/4" I.D. x 11/32" O.D.
Al AND LEAD COLLIMATOR

FIG. 2

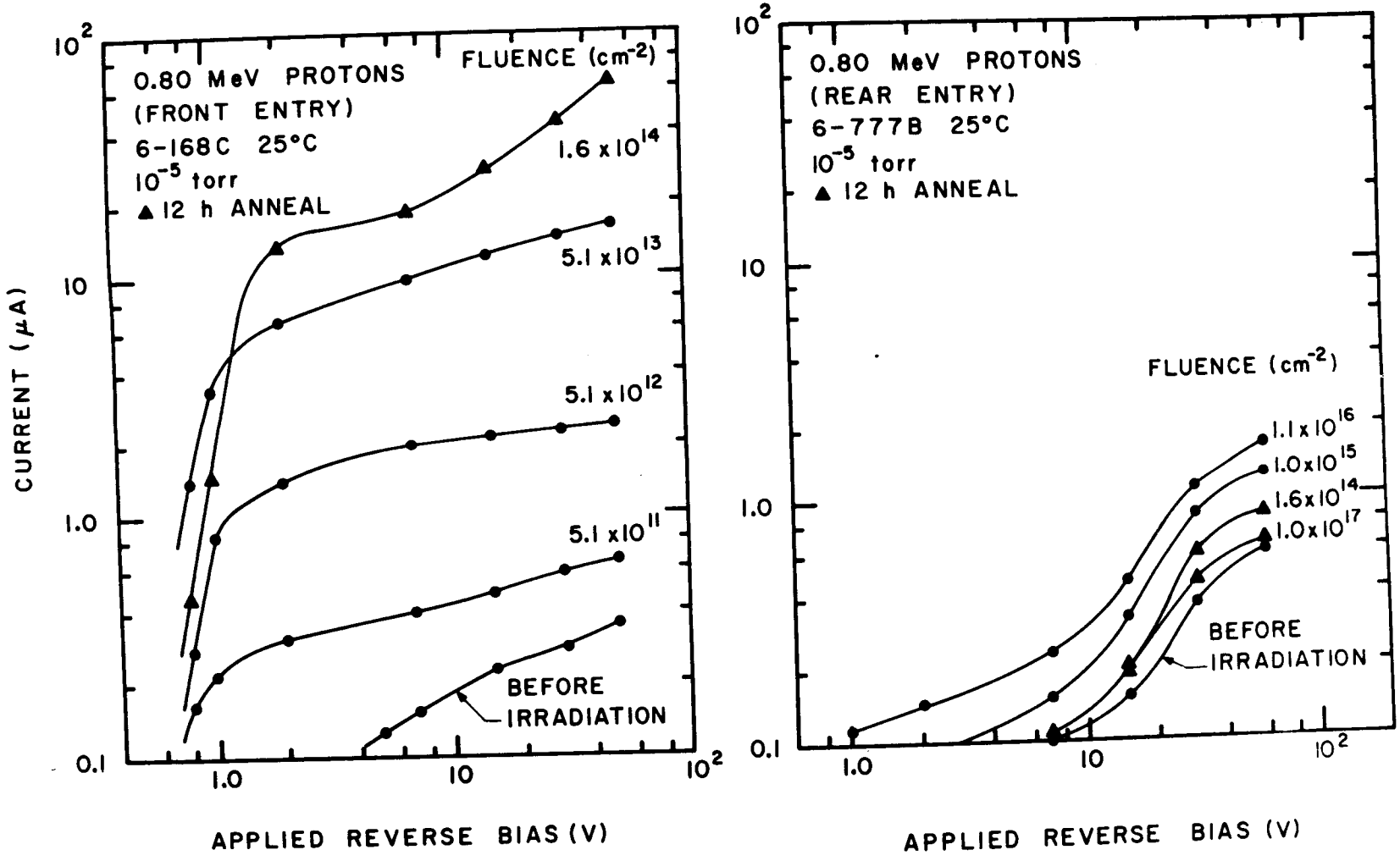
0.80 MeV PROTONS
(FRONT ENTRY)
6-168C 25°C
10^-5 torr
▲ 12 h ANNEAL
FLUENCE (cm^-2)
1.6 x 10^14
5.1 x 10^13
5.1 x 10^12
5.1 x 10^11
BEFORE IRRADIATION
CURRENT (μA)
APPLIED REVERSE BIAS (V)
0.80 MeV PROTONS
(REAR ENTRY)
6-777B 25°C
10^-5 torr
▲ 12 h ANNEAL
FLUENCE (cm^-2)
1.1 x 10^16
1.0 x 10^15
1.6 x 10^14
1.0 x 10^17
BEFORE IRRADIATION
APPLIED REVERSE BIAS (V)

FIG. 3

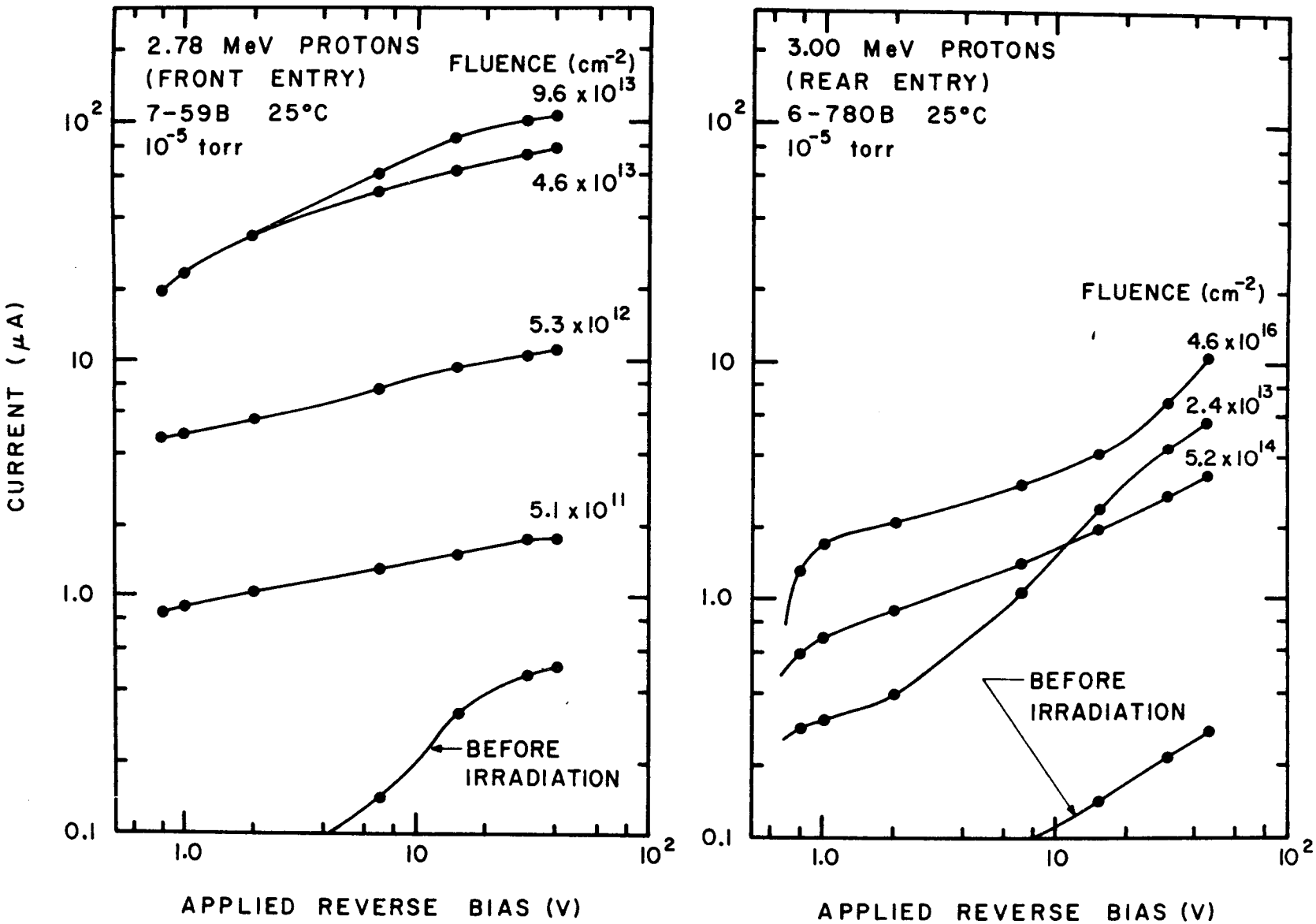
2.78 MeV PROTONS
(FRONT ENTRY)
7-59B 25°C
10^{-5} torr
FLUENCE (cm^{-2})
9.6×10^{13}
4.6×10^{13}
5.3×10^{12}
5.1×10^{11}
BEFORE IRRADIATION
CURRENT (μA)
APPLIED REVERSE BIAS (V)
3.00 MeV PROTONS
(REAR ENTRY)
6-780B 25°C
10^{-5} torr
FLUENCE (cm^{-2})
4.6×10^{16}
2.4×10^{13}
5.2×10^{14}
BEFORE IRRADIATION
APPLIED REVERSE BIAS (V)

FIG. 4

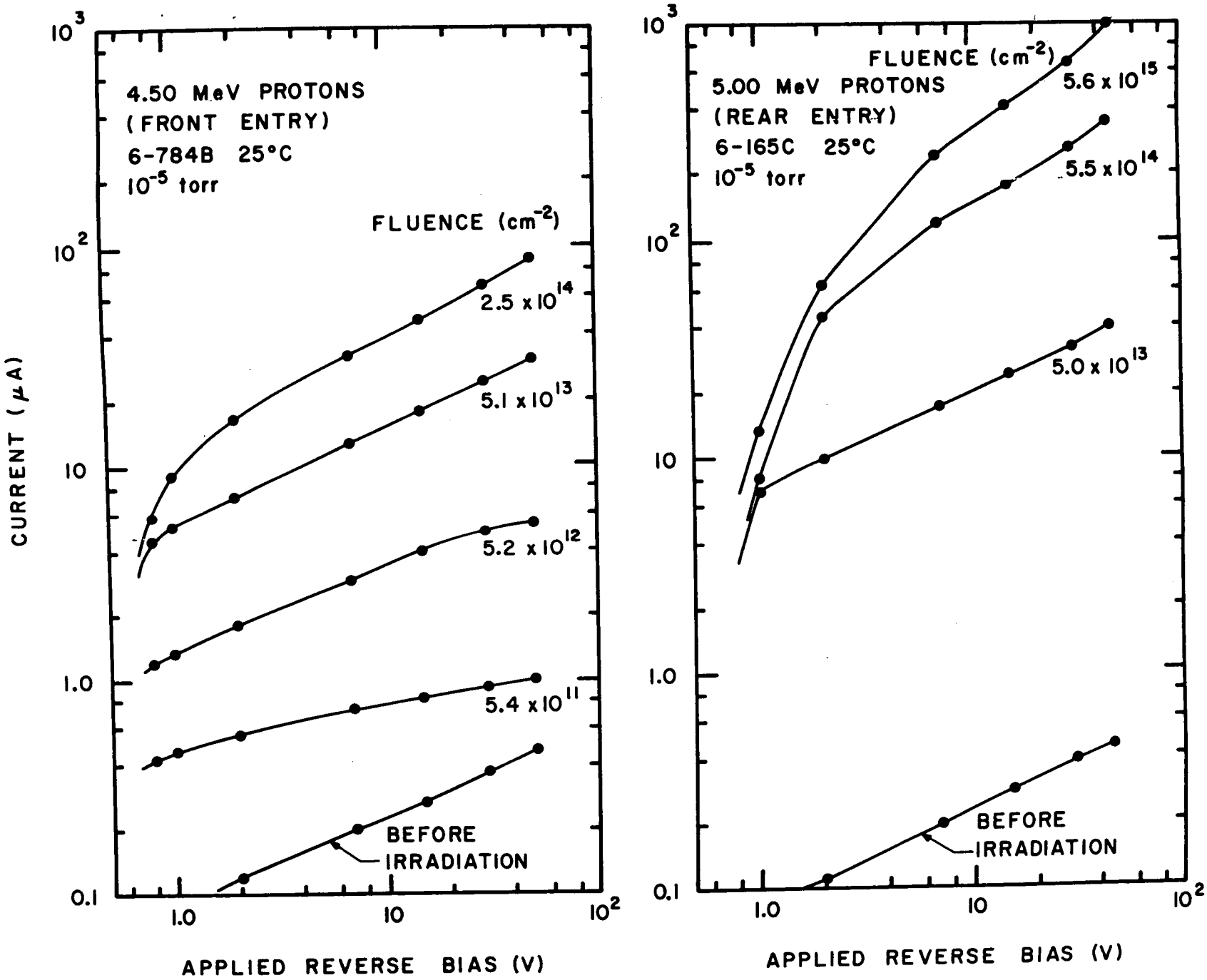
4.50 MeV PROTONS
(FRONT ENTRY)
6-784B 25°C
10^{-5} torr
FLUENCE (cm^{-2})
2.5×10^{14}
5.1×10^{13}
5.2×10^{12}
5.4×10^{11}
BEFORE IRRADIATION
CURRENT (μA)
APPLIED REVERSE BIAS (V)
5.00 MeV PROTONS
(REAR ENTRY)
6-165C 25°C
10^{-5} torr
FLUENCE (cm^{-2})
5.6×10^{15}
5.5×10^{14}
5.0×10^{13}
BEFORE IRRADIATION
APPLIED REVERSE BIAS (V)

FIG. 5

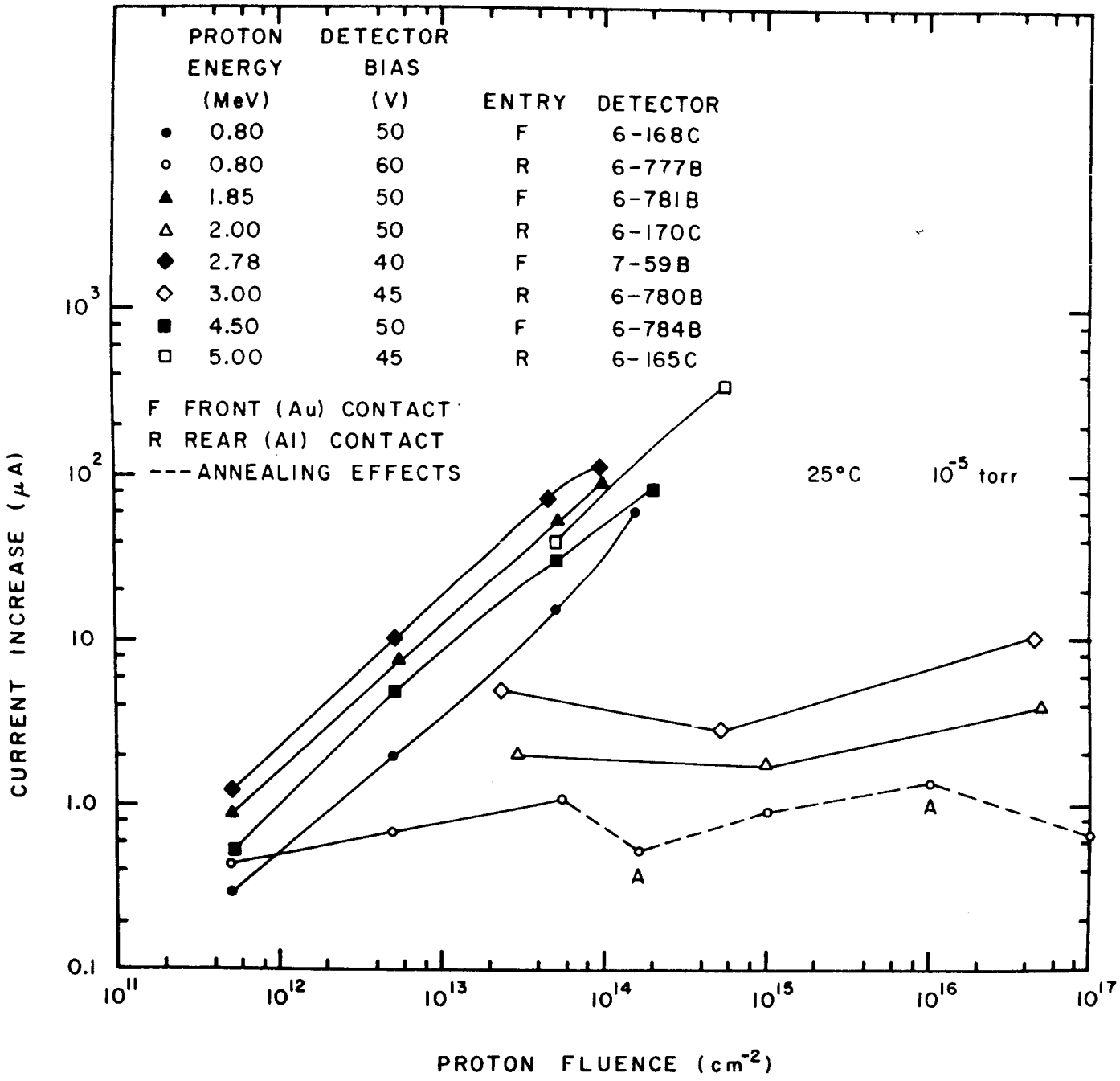
PROTON ENERGY (MeV)
DETECTOR BIAS (V)
ENTRY
DETECTOR
0.80 50 F 6-168C
0.80 60 R 6-777B
1.85 50 F 6-781B
2.00 50 R 6-170C
2.78 40 F 7-59B
3.00 45 R 6-780B
4.50 50 F 6-784B
5.00 45 R 6-165C
F FRONT (Au) CONTACT
R REAR (Al) CONTACT
---ANNEALING EFFECTS
25°C
10^-5 torr
A
A
CURRENT INCREASE (μA)
PROTON FLUENCE (cm^-2)
10^3
10^2
10
1.0
0.1
10^11
10^12
10^13
10^14
10^15
10^16
10^17

FIG. 6

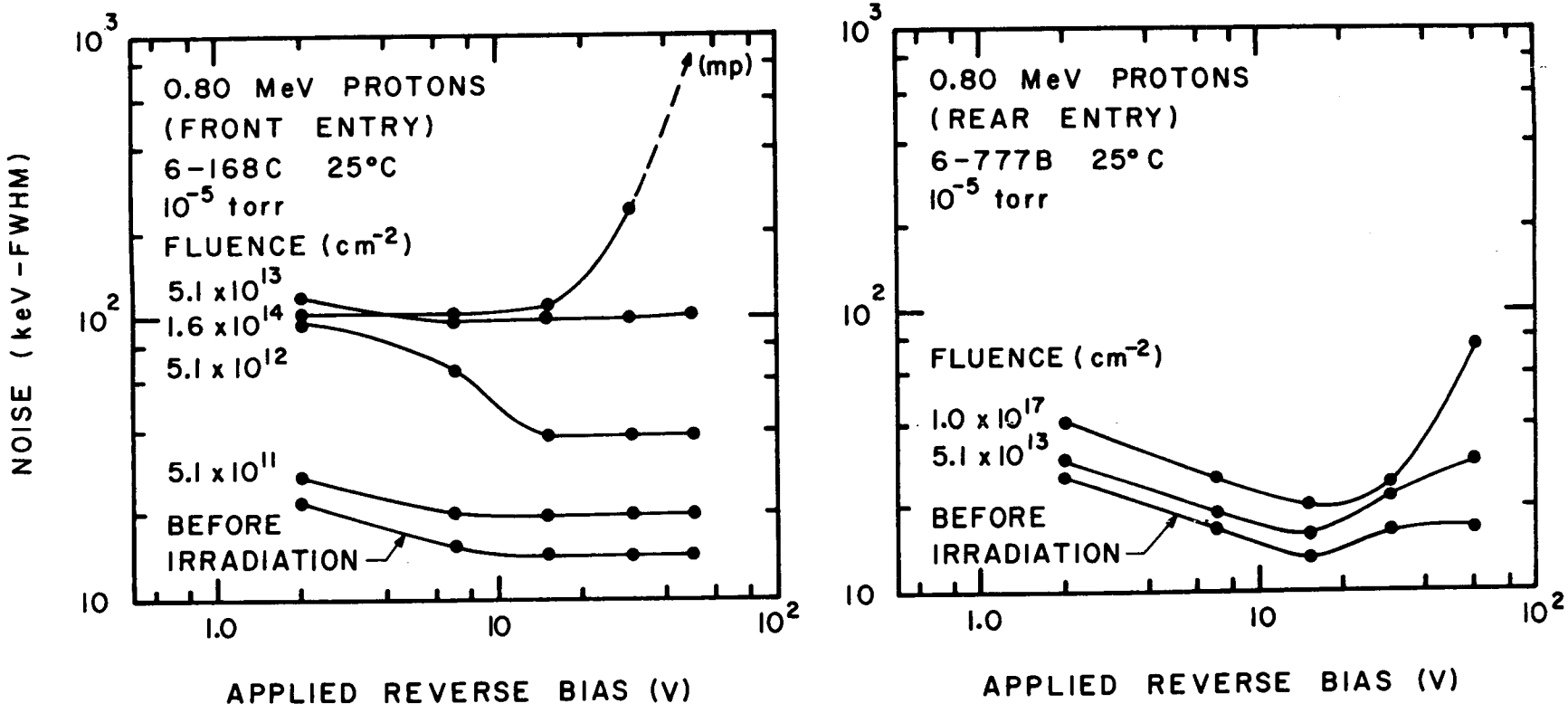
0.80 MeV PROTONS
(FRONT ENTRY)
6-168C 25°C
10^-5 torr
FLUENCE (cm^-2)
5.1 x10^13
1.6 x10^14
5.1 x 10^12
5.1 x10^11
BEFORE
IRRADIATION
(mp)
NOISE (keV-FWHM)
APPLIED REVERSE BIAS (V)
0.80 MeV PROTONS
(REAR ENTRY)
6-777B 25° C
10^-5 torr
FLUENCE (cm^-2)
1.0 x 10^17
5.1 x 10^13
BEFORE
IRRADIATION
APPLIED REVERSE BIAS (V)

FIG. 7

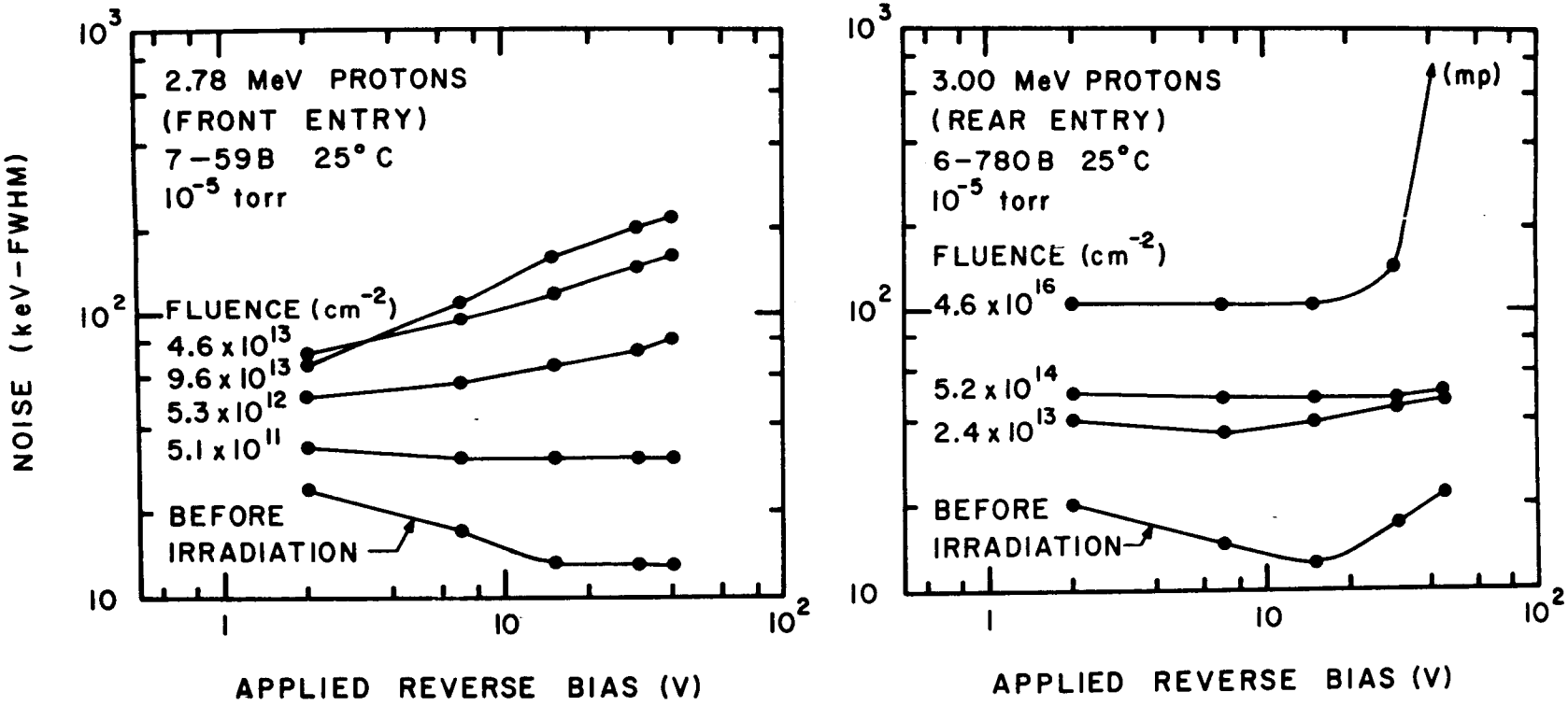
NOISE (keV-FWHM)
2.78 MeV PROTONS
(FRONT ENTRY)
7-59B 25° C
10^-5 torr
FLUENCE (cm^-2)
4.6 x 10^13
9.6 x 10^13
5.3 x 10^12
5.1 x 10^11
BEFORE
IRRADIATION
APPLIED REVERSE BIAS (V)
3.00 MeV PROTONS
(REAR ENTRY)
6-780B 25°C
10^-5 torr
(mp)
FLUENCE (cm^-2)
4.6 x 10^16
5.2 x 10^14
2.4 x 10^13
BEFORE
IRRADIATION
APPLIED REVERSE BIAS (V)

FIG.8

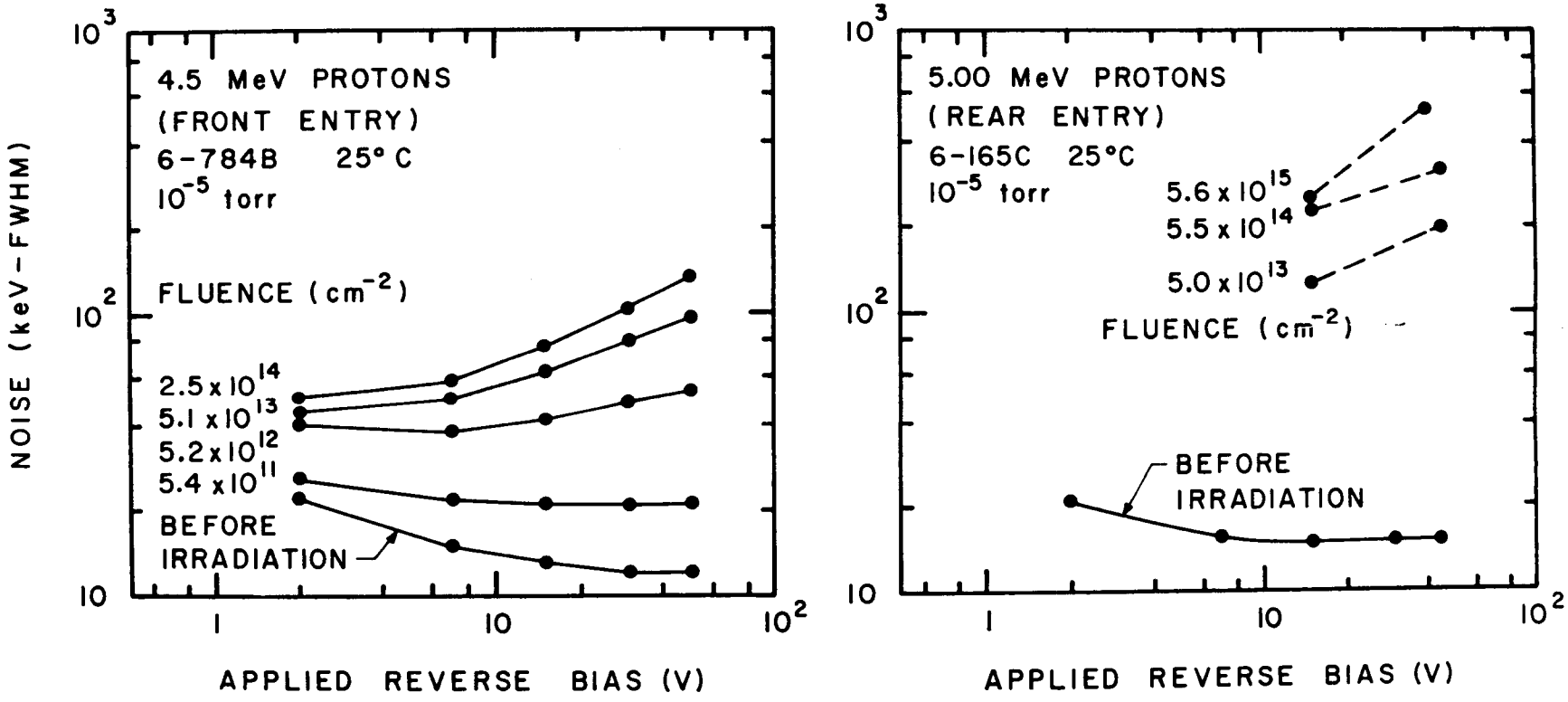
4.5 MeV PROTONS
(FRONT ENTRY)
6-784B 25° C
10^-5 torr
FLUENCE (cm^-2)
2.5 x 10^14
5.1 x 10^13
5.2 x 10^12
5.4 x 10^11
BEFORE IRRADIATION
NOISE (keV-FWHM)
APPLIED REVERSE BIAS (V)
5.00 MeV PROTONS
(REAR ENTRY)
6-165C 25°C
10^-5 torr
5.6 x 10^15
5.5 x 10^14
5.0 x 10^13
FLUENCE (cm^-2)
BEFORE IRRADIATION
APPLIED REVERSE BIAS (V)

FIG. 9

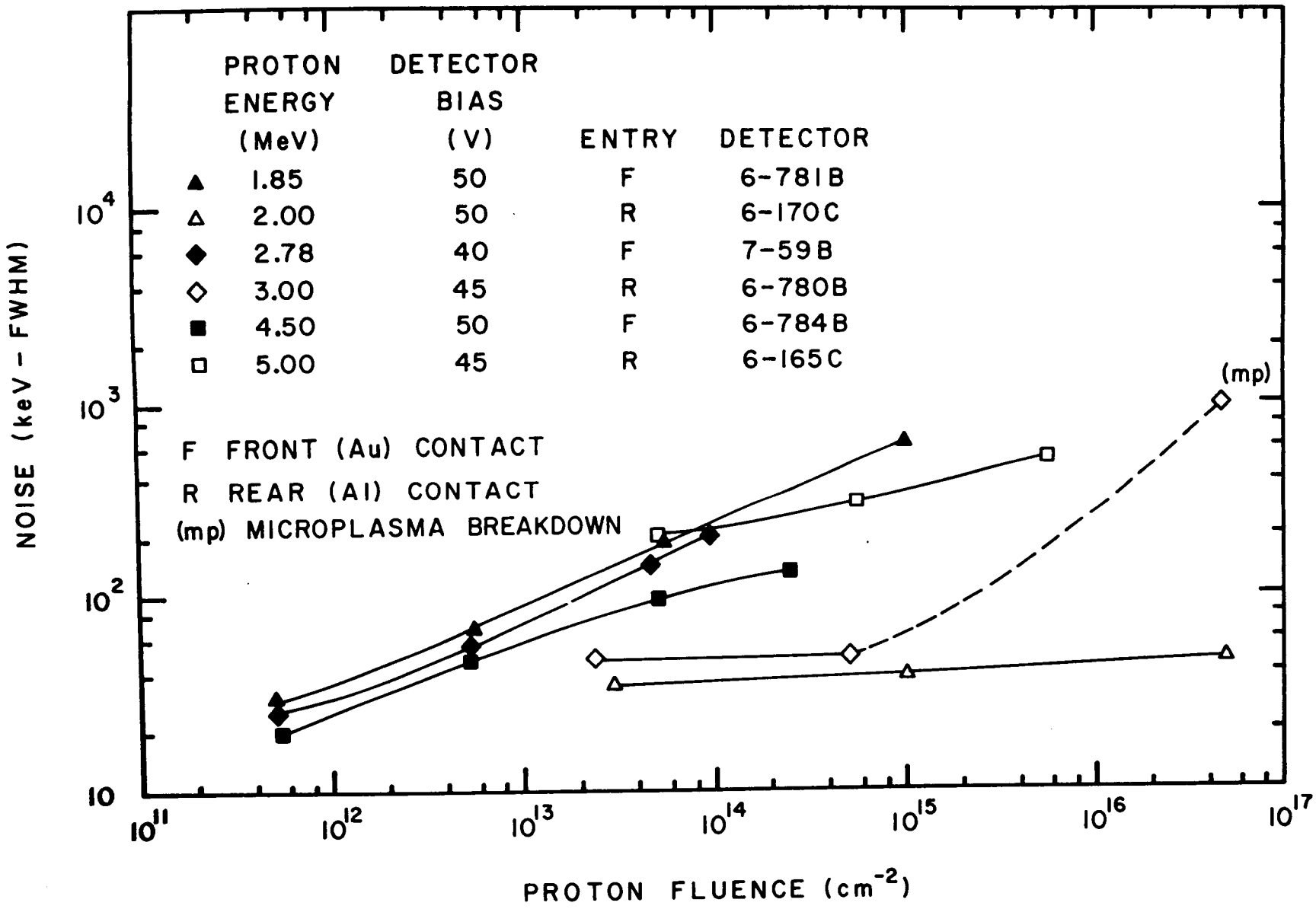
PROTON ENERGY (MeV)
DETECTOR BIAS (V)
ENTRY
DETECTOR
1.85 50 F 6-781B
2.00 50 R 6-170C
2.78 40 F 7-59B
3.00 45 R 6-780B
4.50 50 F 6-784B
5.00 45 R 6-165C
F FRONT (Au) CONTACT
R REAR (Al) CONTACT
(mp) MICROPLASMA BREAKDOWN
(mp)
NOISE (keV - FWHM)
PROTON FLUENCE (cm^{-2})
10
10^2
10^3
10^4
10^{11}
10^{12}
10^{13}
10^{14}
10^{15}
10^{16}
10^{17}

FIG. 10

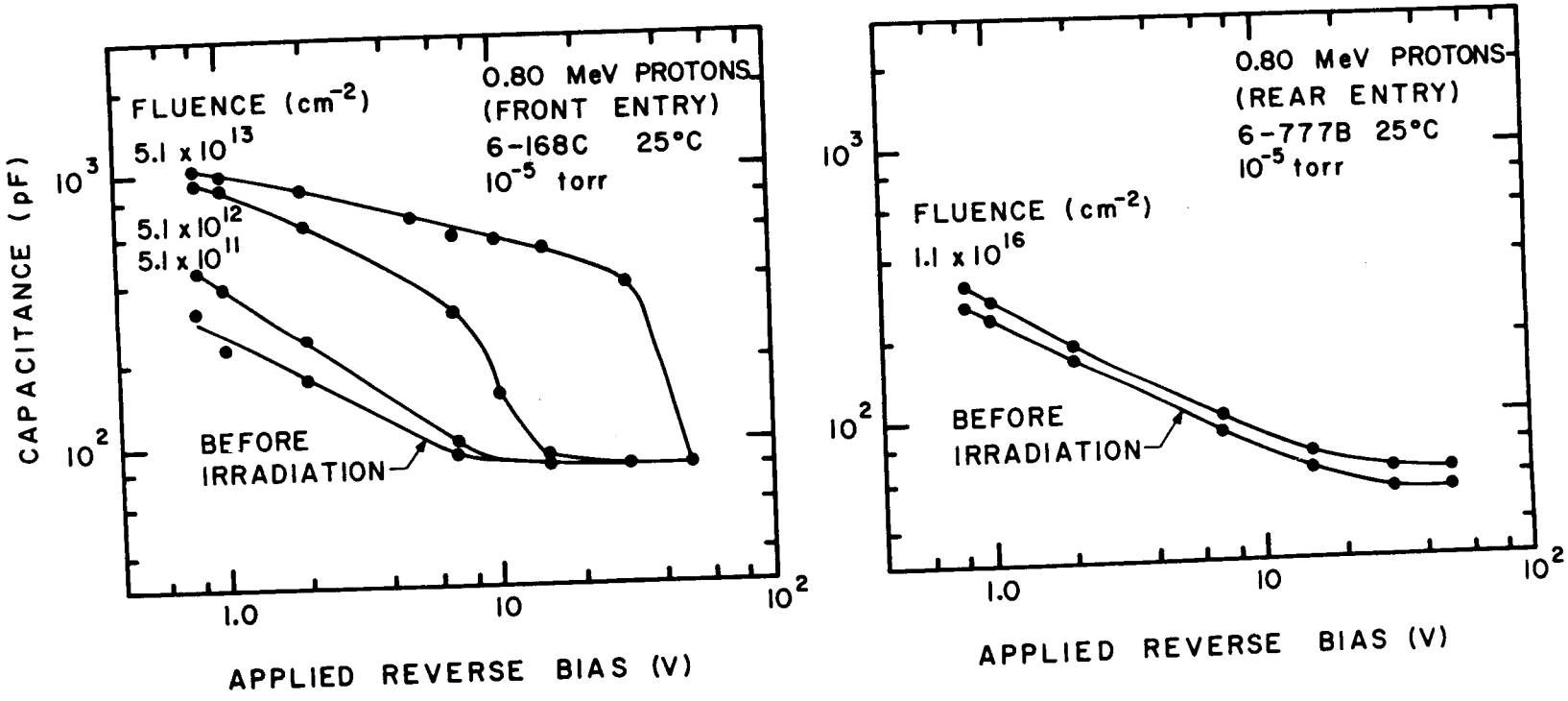
CAPACITANCE (pF)
10^3
10^2
FLUENCE (cm^{-2})
5.1×10^{13}
5.1×10^{12}
5.1×10^{11}
0.80 MeV PROTONS
(FRONT ENTRY)
6-168C 25°C
10^{-5} torr
BEFORE
IRRADIATION
1.0
10
10^2
APPLIED REVERSE BIAS (V)
10^3
10^2
0.80 MeV PROTONS
(REAR ENTRY)
6-777B 25°C
10^{-5} torr
FLUENCE (cm^{-2})
1.1×10^{16}
BEFORE
IRRADIATION
1.0
10
10^2
APPLIED REVERSE BIAS (V)

FIG. 11

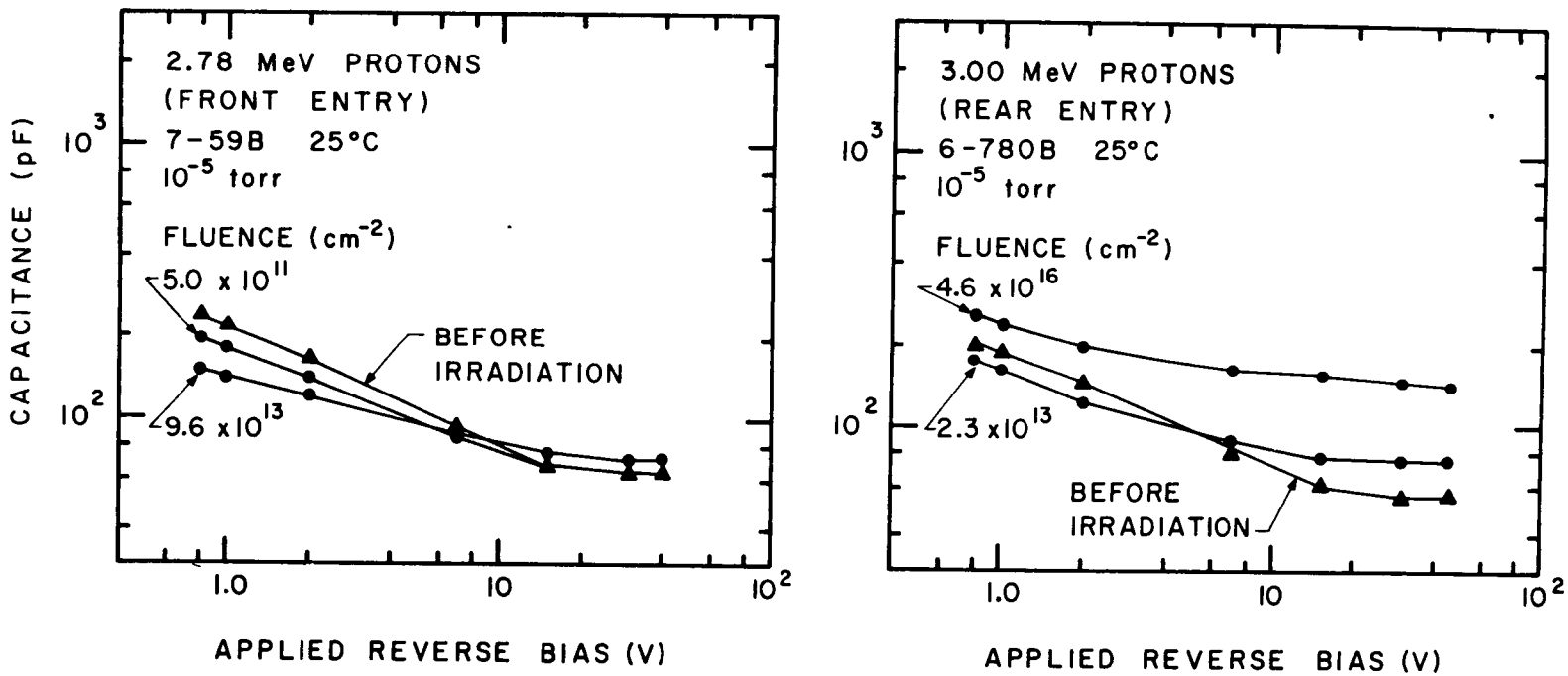
2.78 MeV PROTONS
(FRONT ENTRY)
7-59B 25°C
10^-5 torr
FLUENCE (cm^-2)
5.0 x 10^11
9.6 x 10^13
BEFORE IRRADIATION
CAPACITANCE (pF)
10^3
10^2
1.0
10
10^2
APPLIED REVERSE BIAS (V)
3.00 MeV PROTONS
(REAR ENTRY)
6-780B 25°C
10^-5 torr
FLUENCE (cm^-2)
4.6 x 10^16
2.3 x 10^13
BEFORE IRRADIATION
10^3
10^2
1.0
10
10^2
APPLIED REVERSE BIAS (V)

FIG. 12

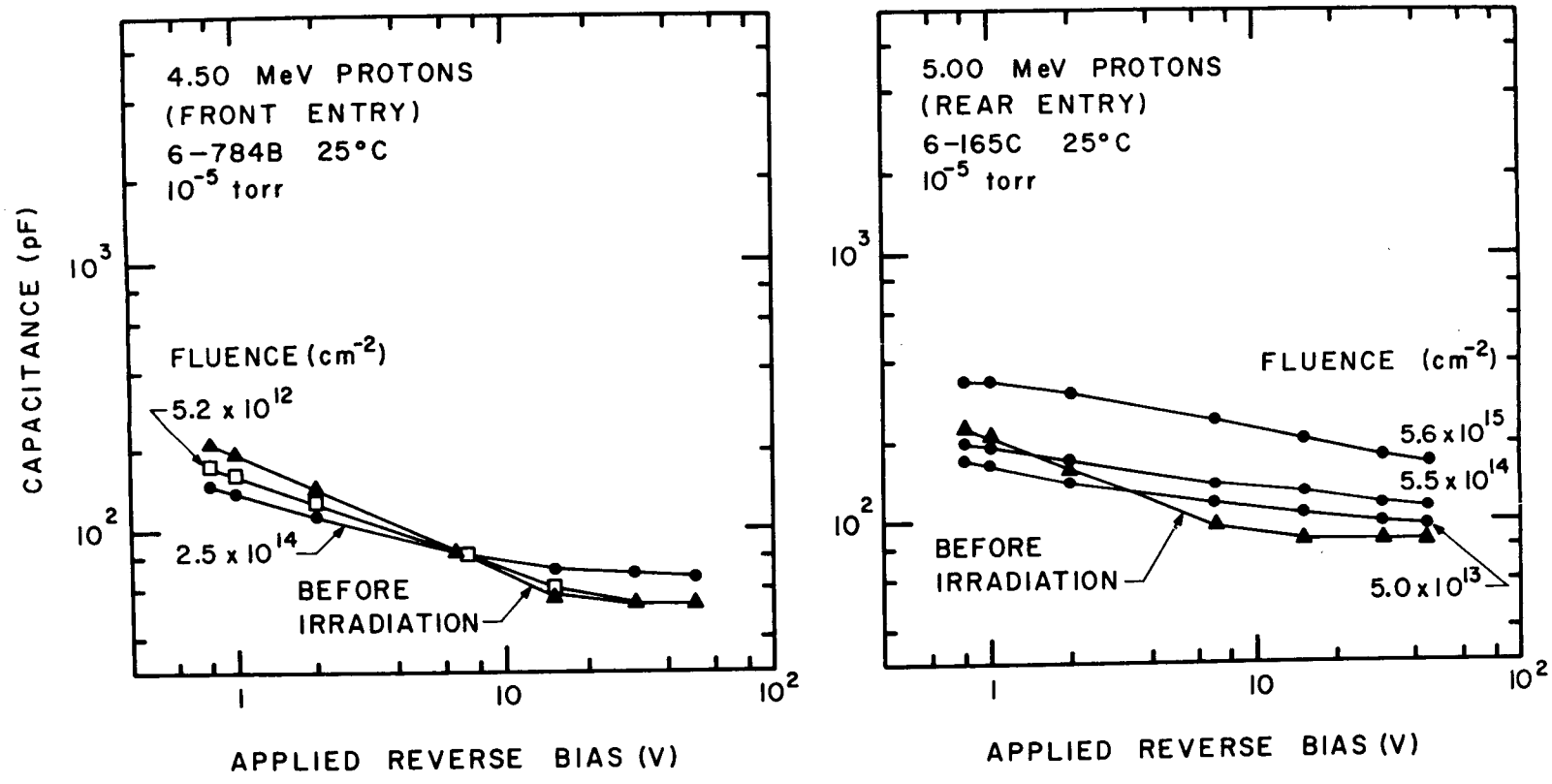
4.50 MeV PROTONS
(FRONT ENTRY)
6-784B 25°C
10^-5 torr
FLUENCE (cm^-2)
5.2 x 10^12
2.5 x 10^14
BEFORE
IRRADIATION
CAPACITANCE (pF)
10^3
10^2
1
10
10^2
APPLIED REVERSE BIAS (V)
5.00 MeV PROTONS
(REAR ENTRY)
6-165C 25°C
10^-5 torr
FLUENCE (cm^-2)
5.6 x 10^15
5.5 x 10^14
5.0 x 10^13
BEFORE
IRRADIATION
10^3
10^2
1
10
10^2
APPLIED REVERSE BIAS (V)

FIG. 13

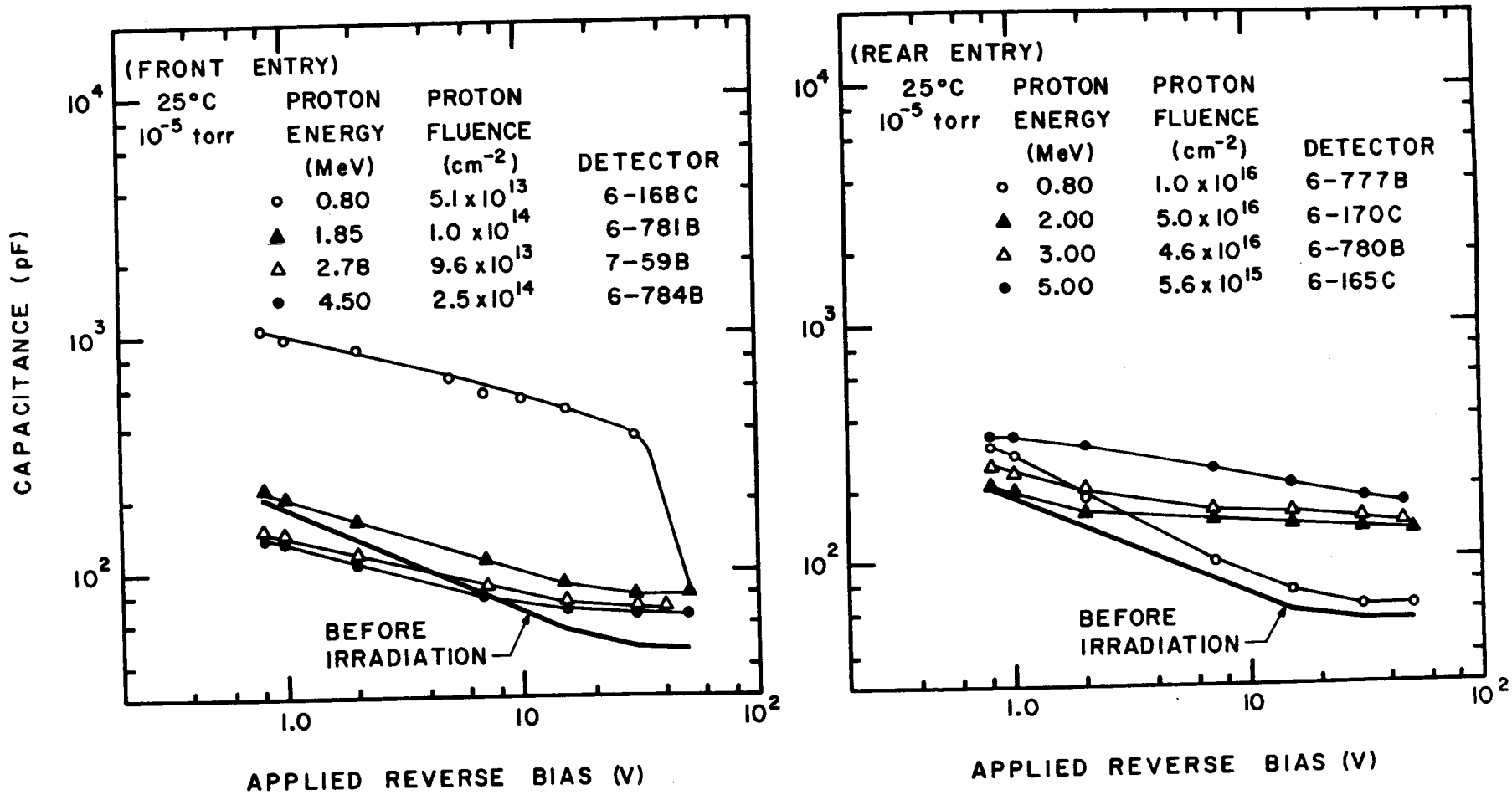
(FRONT ENTRY)
25°C
10^-5 torr
PROTON ENERGY (MeV)
PROTON FLUENCE (cm^-2)
DETECTOR
0.80 5.1 x 10^13 6-168C
1.85 1.0 x 10^14 6-781B
2.78 9.6 x 10^13 7-59B
4.50 2.5 x 10^14 6-784B
BEFORE IRRADIATION
CAPACITANCE (pF)
APPLIED REVERSE BIAS (V)
(REAR ENTRY)
25°C
10^-5 torr
PROTON ENERGY (MeV)
PROTON FLUENCE (cm^-2)
DETECTOR
0.80 1.0 x 10^16 6-777B
2.00 5.0 x 10^16 6-170C
3.00 4.6 x 10^16 6-780B
5.00 5.6 x 10^15 6-165C
BEFORE IRRADIATION
APPLIED REVERSE BIAS (V)

FIG.14

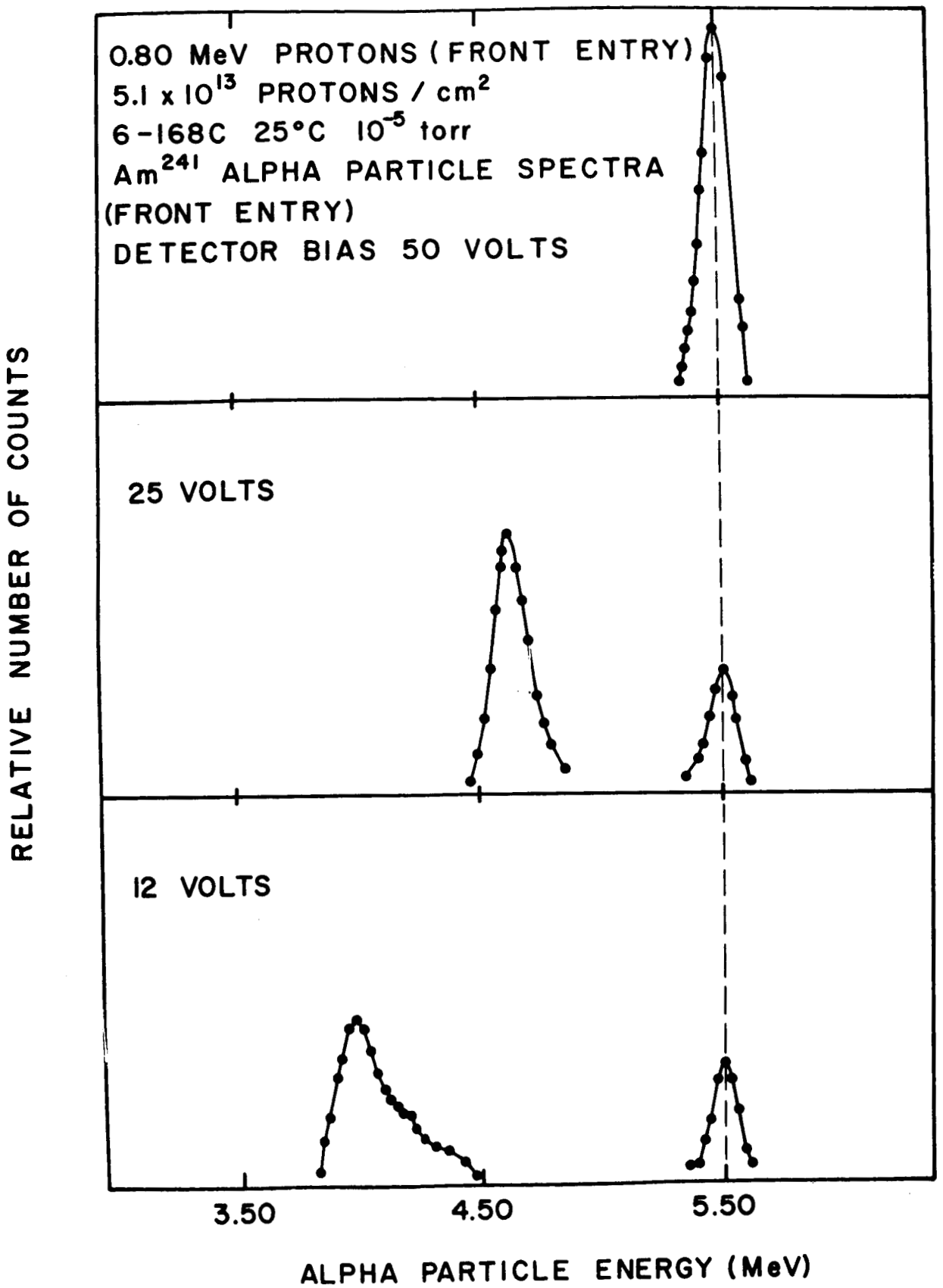
0.80 MeV PROTONS (FRONT ENTRY)
5.1 x 10^13 PROTONS / cm^2
6-168C 25°C 10^-5 torr
Am^241 ALPHA PARTICLE SPECTRA
(FRONT ENTRY)
DETECTOR BIAS 50 VOLTS
25 VOLTS
12 VOLTS
RELATIVE NUMBER OF COUNTS
3.50
4.50
5.50
ALPHA PARTICLE ENERGY (MeV)

FIG. 15

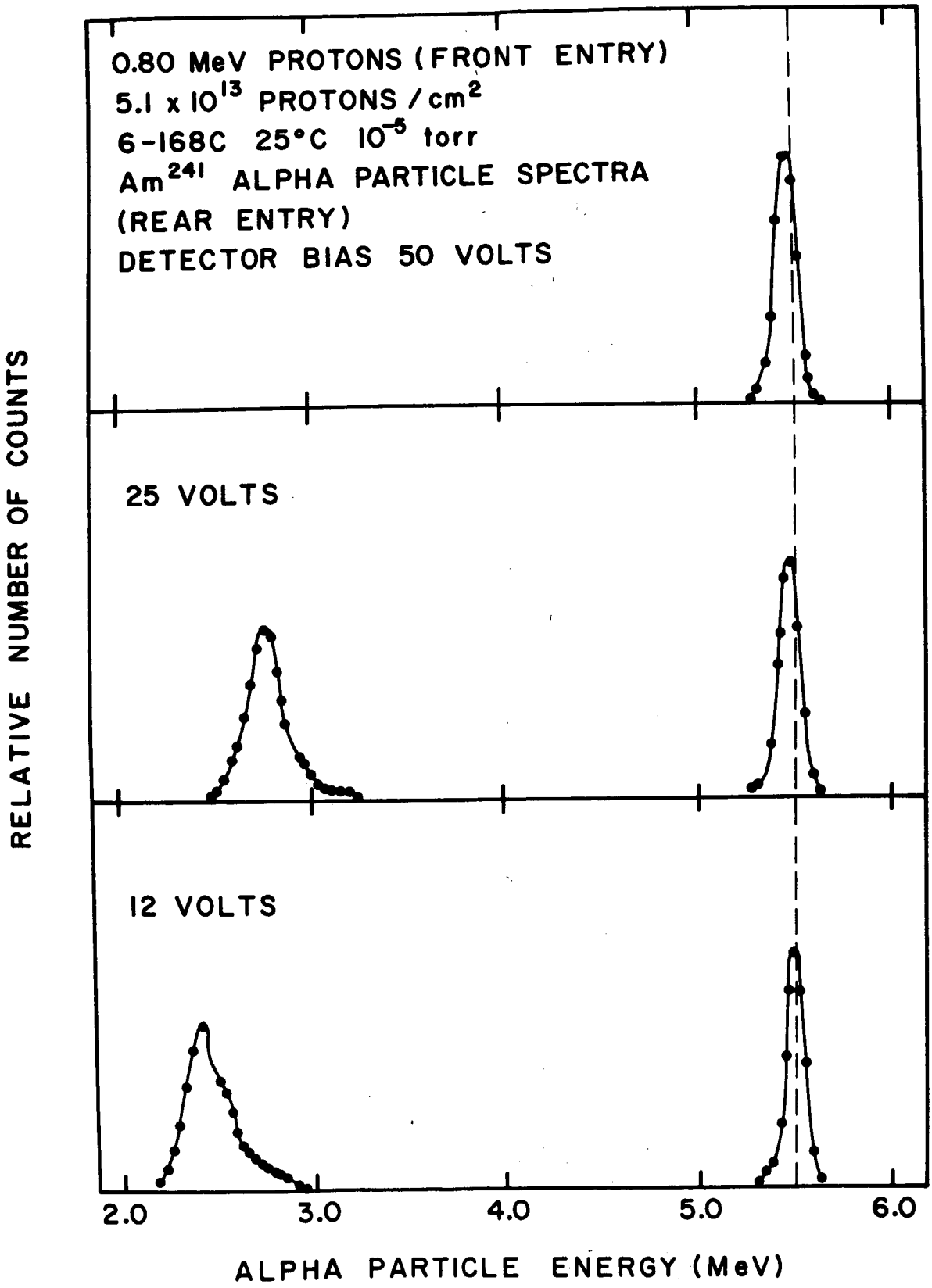
0.80 MeV PROTONS (FRONT ENTRY)
5.1 x 10^13 PROTONS / cm^2
6-168C 25°C 10^-5 torr
Am^241 ALPHA PARTICLE SPECTRA
(REAR ENTRY)
DETECTOR BIAS 50 VOLTS
25 VOLTS
12 VOLTS
RELATIVE NUMBER OF COUNTS
2.0
3.0
4.0
5.0
6.0
ALPHA PARTICLE ENERGY (MeV)

FIG. 16

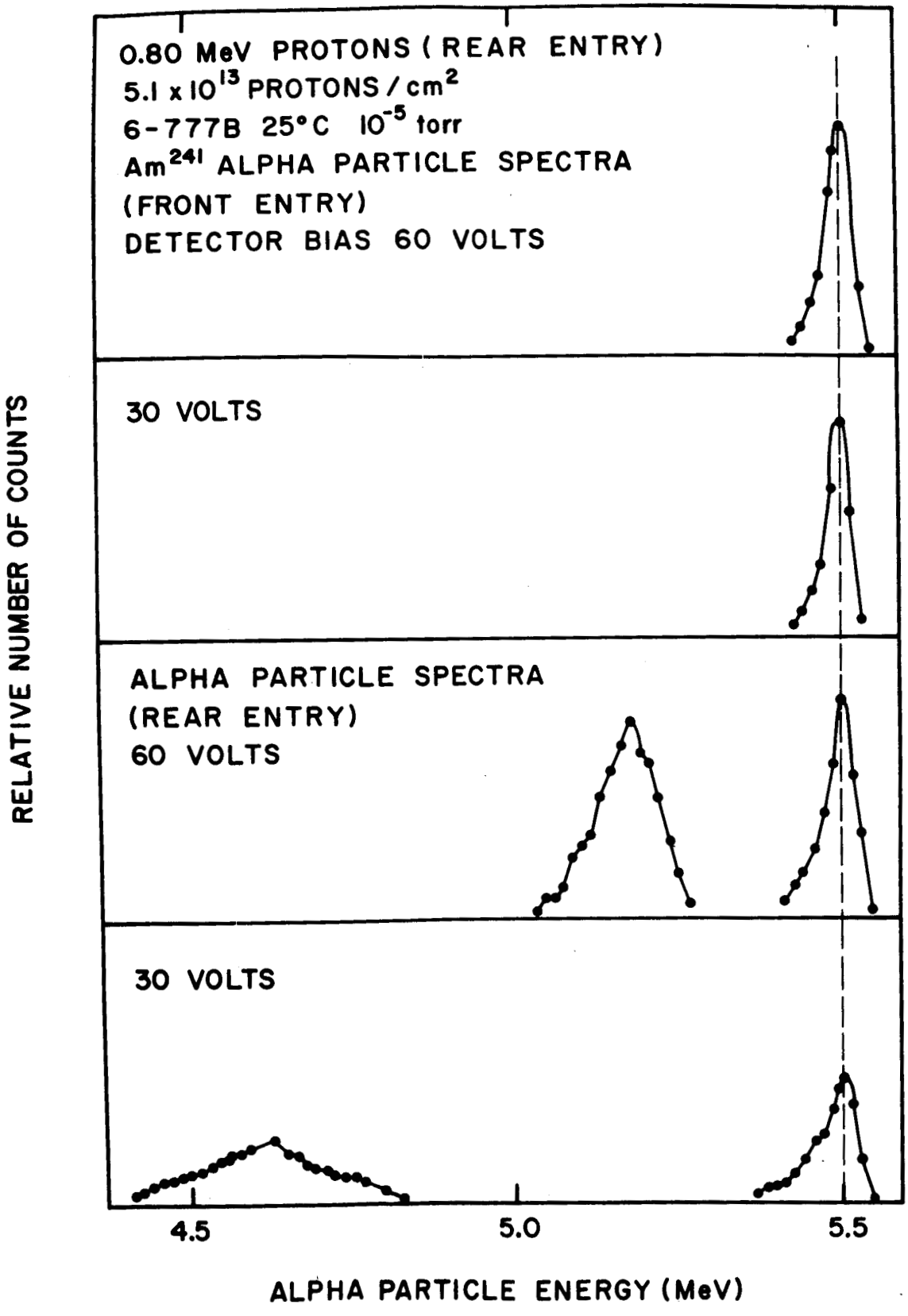
0.80 MeV PROTONS (REAR ENTRY)
5.1 x 10^13 PROTONS / cm^2
6-777B 25°C 10^-5 torr
Am^241 ALPHA PARTICLE SPECTRA
(FRONT ENTRY)
DETECTOR BIAS 60 VOLTS
30 VOLTS
ALPHA PARTICLE SPECTRA
(REAR ENTRY)
60 VOLTS
30 VOLTS
RELATIVE NUMBER OF COUNTS
4.5
5.0
5.5
ALPHA PARTICLE ENERGY (MeV)

FIG. 17

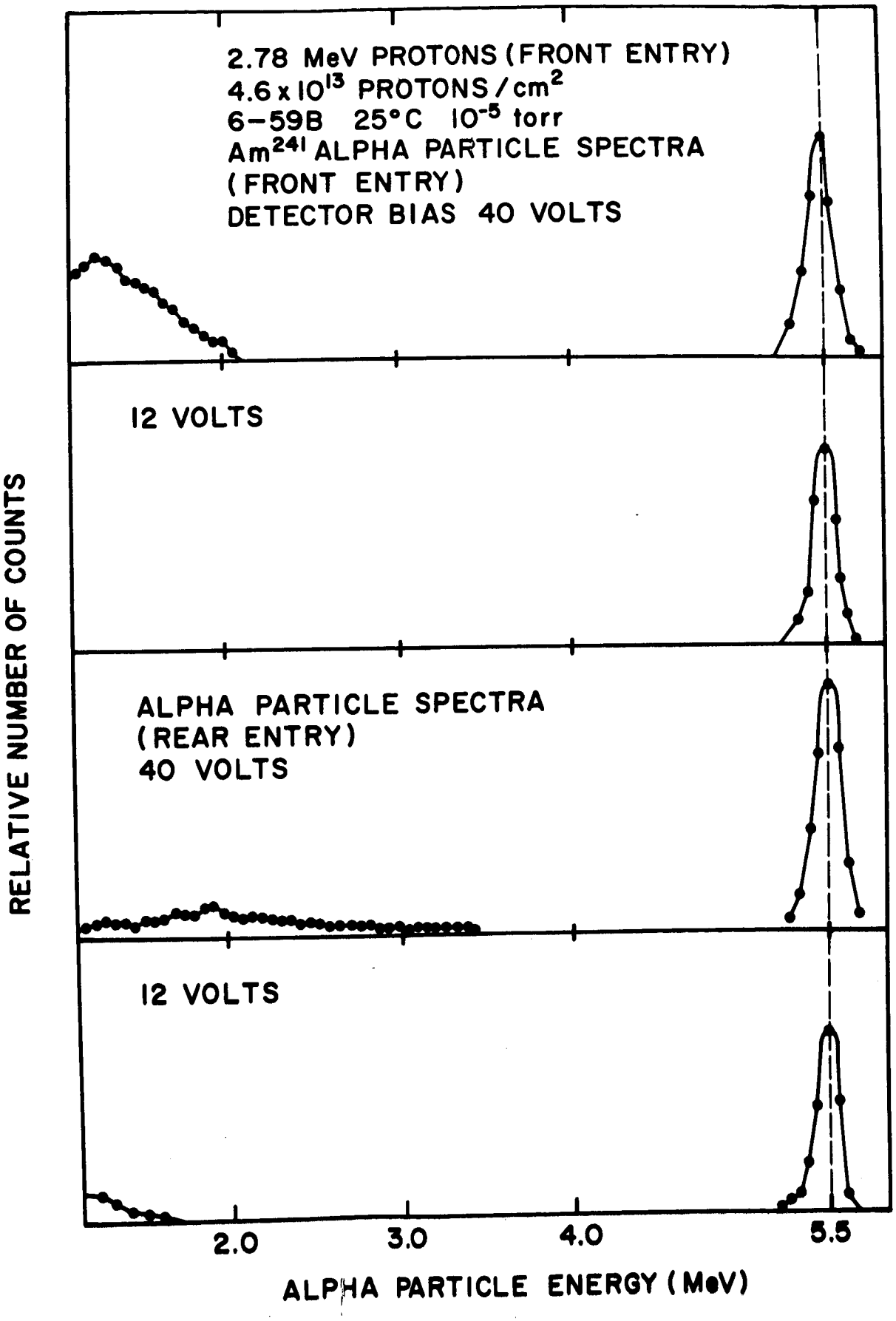
2.78 MeV PROTONS (FRONT ENTRY)
4.6 x 10^13 PROTONS / cm^2
6-59B 25°C 10^-5 torr
Am^241 ALPHA PARTICLE SPECTRA
(FRONT ENTRY)
DETECTOR BIAS 40 VOLTS
12 VOLTS
ALPHA PARTICLE SPECTRA
(REAR ENTRY)
40 VOLTS
12 VOLTS
RELATIVE NUMBER OF COUNTS
2.0
3.0
4.0
5.5
ALPHA PARTICLE ENERGY (MeV)

FIG. 18

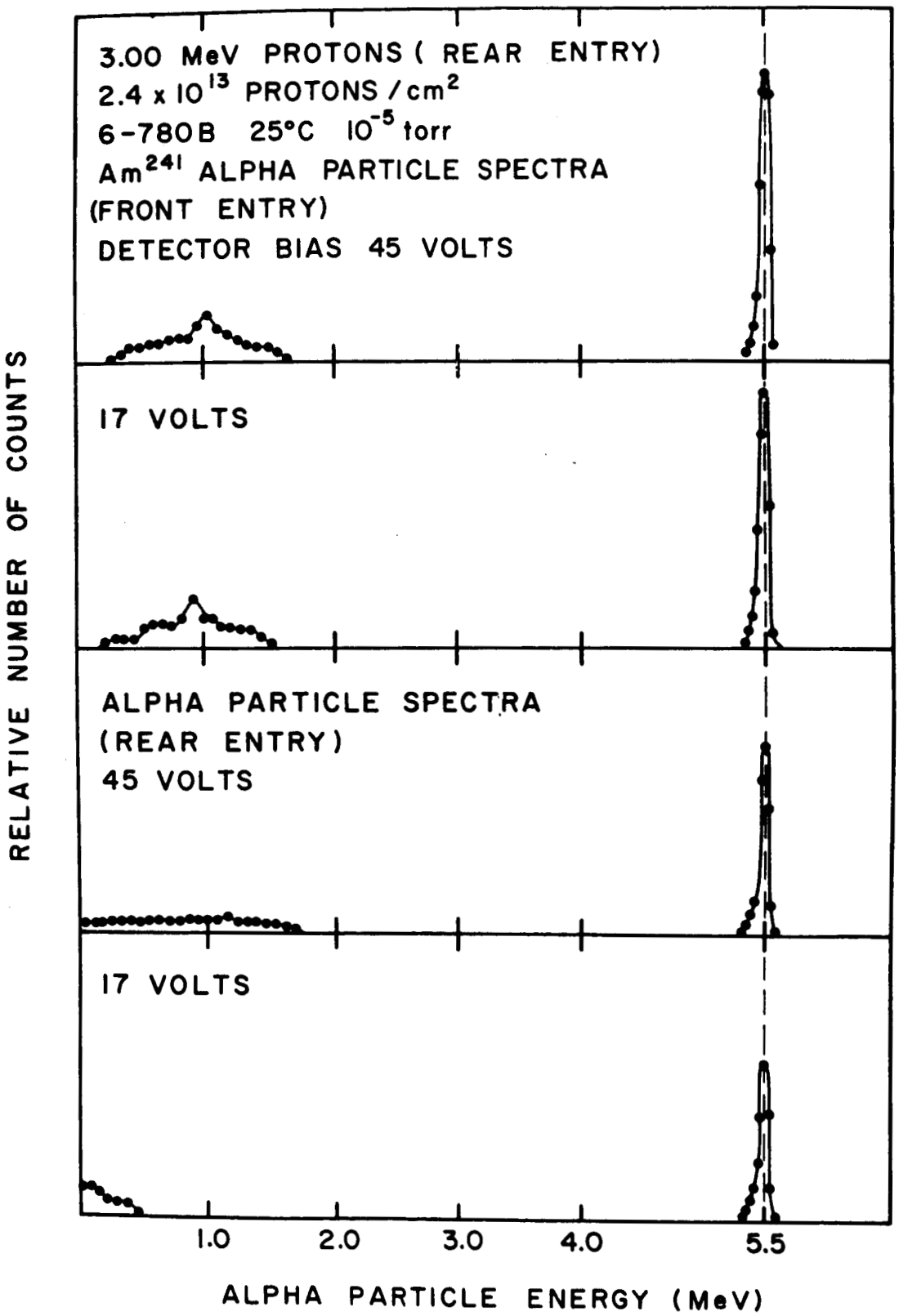
3.00 MeV PROTONS (REAR ENTRY)
2.4 x 10^13 PROTONS / cm^2
6-780B 25°C 10^-5 torr
Am^241 ALPHA PARTICLE SPECTRA
(FRONT ENTRY)
DETECTOR BIAS 45 VOLTS
17 VOLTS
ALPHA PARTICLE SPECTRA
(REAR ENTRY)
45 VOLTS
17 VOLTS
RELATIVE NUMBER OF COUNTS
1.0
2.0
3.0
4.0
5.5
ALPHA PARTICLE ENERGY (MeV)

FIG. 19

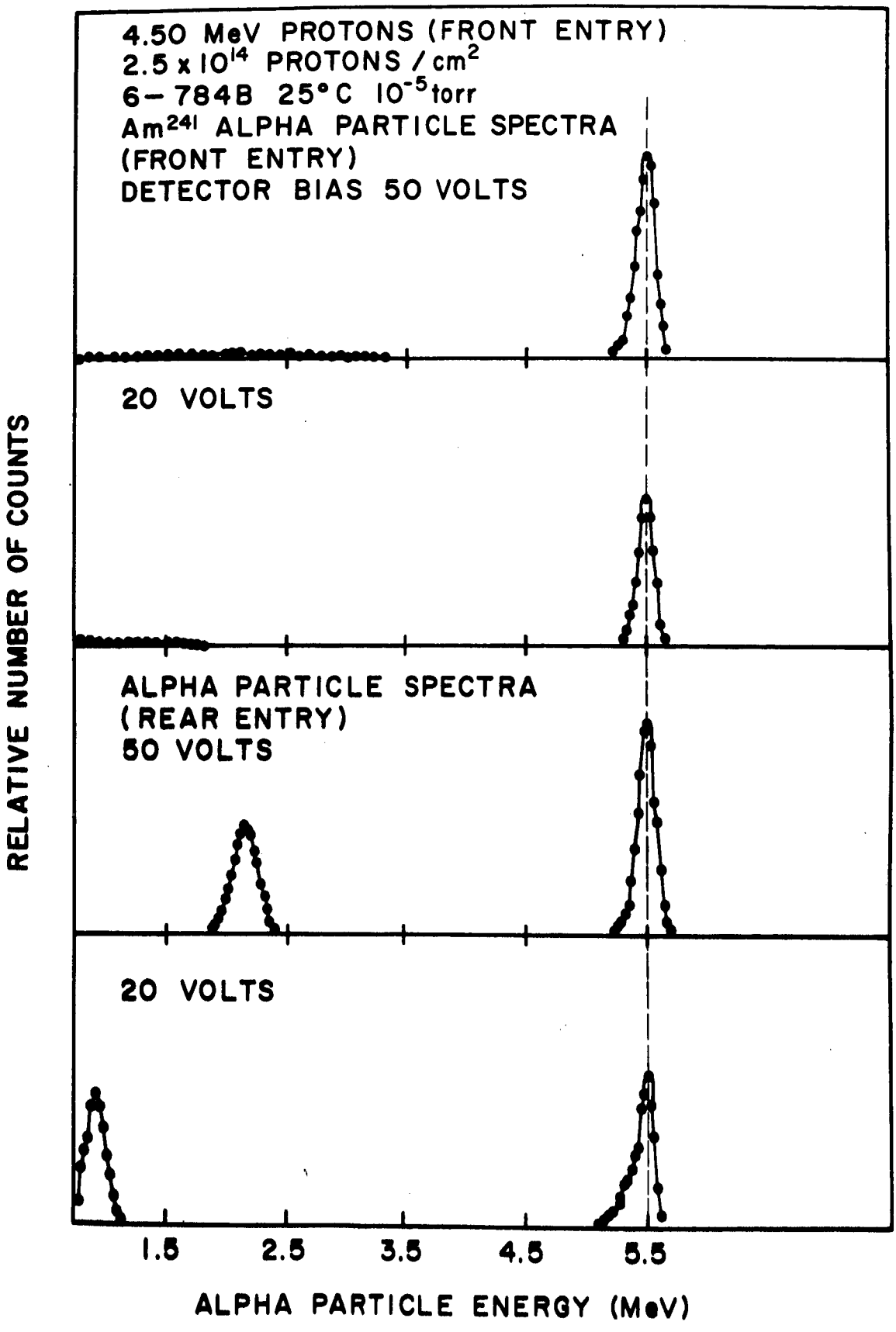
4.50 MeV PROTONS (FRONT ENTRY)
2.5 x 10^14 PROTONS / cm^2
6-784B 25°C 10^-5 torr
Am^241 ALPHA PARTICLE SPECTRA
(FRONT ENTRY)
DETECTOR BIAS 50 VOLTS
20 VOLTS
ALPHA PARTICLE SPECTRA
(REAR ENTRY)
50 VOLTS
20 VOLTS
RELATIVE NUMBER OF COUNTS
1.5
2.5
3.5
4.5
5.5
ALPHA PARTICLE ENERGY (MeV)

FIG. 20